SCIENTIFIC HIGHLIGHTS

The following articles show a sampling of the main topics of research at DIPC.

2004/05

Deconfinement In a Two-dimensional Optical Lattice

by *A.F. Ho*[1], *M.A. Cazalilla*[2] *and T. Giamarchi*[3]

As it was experimentally demonstrated ten years ago, in three dimensional space, bosons can undergo Bose-Einstein condensation, that is, they can reside in the same quantum state. However, when confined in a one-dimensional structure, such a phenomenon becomes impossible. Furthermore, a periodic potential and boson-boson interactions can both conspire to localize the atoms in an insulating state known as Mott insulator. We investigate how the transition between these different states takes place in a system of bosonic atoms confined in an anisotropic optical lattice.

In 1924, Albert Einstein received a letter from an entirely unknown Indian physicist, S.N. Bose. By that time, Einstein had been already awarded a Nobel prize, and was well known and famous even to the general public. Enclosed with Bose's letter, there was a manuscript, for which Bose requested Einstein's assistance for its translation and submission to a renowned German journal, *Zeitschrift für Physik*. In his manuscript, Bose presented a statistical method that he applied to the study of radiation, demonstrating how to obtain Planck's radiation formulas from the basic assumption of the existence of light quanta ("photons") put forward by Einstein himself twenty years earlier. Einstein quickly realized the importance of the work of his Indian colleague, and not only did he prepare a translation and submitted it to the journal, but also found a nice extension to Bose's work. This is how he came across the phenomenon called Bose-Einstein condensation (BEC): Einstein noticed that, by applying Bose's statistical rules to atoms (instead of photons, as Bose had done), the atoms should undergo an interesting transition at sufficiently low temperatures. Indeed, whereas at high enough temperature a gas of atoms described by Bose statistics would entirely behave as a classical gas, as the temperature decreases, the behavior would become qualitatively different, and eventually, below a certain temperature, most of the atoms would reside in the same (quantum) state. Almost seventy years later, BEC was observed in a diluted gas of alkali atoms, cooled down to temperatures of about one millionth of degree above the absolute zero (–273.16 degrees Celsius). It happened just as Einstein had predicted using Bose's methods.

Nevertheless, it is interesting to note that Einstein's results apply only for an atomic gas in three spatial dimensions (3D). When one examines the conditions for Bose-Einstein condensation for a gas confined to move in a narrow tube, that is, in one dimension (1D), one reaches the surprising conclusion that BEC cannot occur. In fact, if atoms did not interact at all, BEC would only happen exactly at the absolute zero of temperature. However, with interactions things get worse, since they make the motion of all atoms in 1D correlated, pretty much like the motion of cars in a traffic jam is correlated. As a consequence, BEC in 1D cannot take place even at the absolute zero. However, in view of the above discussion, one question immediately arises: What happens when we go from 1D to 3D? First we have to think of a set up where such an experiment can be done. Miraculously, this has been rendered possible recently thanks to advances in laser manipulation of the same cold alkali gases where BEC was observed in 1995. During the last few years, several experimental groups in Europe and the US have been able to create light interference patterns (a sort of hologram) where one can tightly trap alkali gas atoms in tubes, thus confining their motion to 1D. The force that confines the atoms arises due to the AC Stark effect, i.e. the laser electric field induces a dipole on the atom, which in turn responds to the same electric field by moving to regions where the electric field is low (or large, depending on the laser frequency). The confinement thus attained can be made very tight, such that atoms cannot escape from the tubes but, by decreasing the intensity of the lasers that create the hologram, hopping of atoms from tube to tube can be allowed.

In our article, we mapped out the possible phases (i.e. states of matter) of such a system of weakly coupled tubes. The results uncover the astonishing behavior of strongly correlated quantum matter that can only be observed at temperatures very close to the absolute zero. The competition between the tendency of atoms to gain kinetic energy, and therefore become delocalized, and the tendency to become localized due to their mutual interaction is exhibited by the different phases where the system can be found. We find that not only can the system become a very exotic type of Bose-Einstein condensate (denoted SF in the figure), with very anisotropic properties, but it also exhibits two kinds of Mott insulating phases (1D MI and 2D MI), where the behavior of atoms is dominated by their mutual interactions. What is interesting about cold atomic gases in optical lattices is that the parameters of the system can be changed in a continuous and highly controllable way. Thus, almost at the same time that we carried out our calculations, Tilman Esslinger and his group at the legendary ETH in Zurich (the place from where Einstein himself got his BS and PhD degrees in Physics) were carrying careful experiments that demonstrated that the phases that we predicted are actually observed in the experimental systems. ■

REFERENCE
A.F. Ho, M.A. Cazalilla, and T. Giamarchi, *Physical Review Letters* **92**, 130405 (2004).

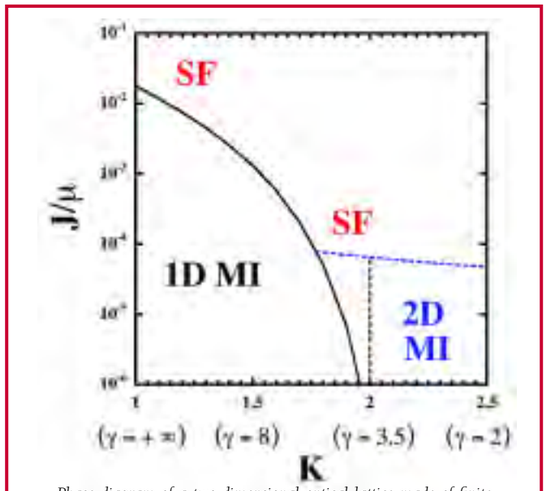

Phase diagram of a two-dimensional optical lattice made of finite one-dimensional gas tubes filled with bosonic atoms. The region labeled SF corresponds to parameter range where an anisotropic Bose-Einstein condensate is stable. The region labeled as 1D MI corresponds to the Mott insulating phase, where atoms are localized at the minima of a periodic potential. The 2D MI phase corresponds to a state where the atoms are localized within the gas tubes, but not by the periodic potential.

We find that not only can the system become a very exotic type of Bose-Einstein condensate, with very anisotropic properties, but it also exhibits two kinds of Mott insulating phases, where the behavior of atoms is dominated by their mutual interactions.

1 School of Physics and Astronomy, The University of Birmingham, Edgbaston, UK
2 Donostia International Physics Center, San Sebastian, Spain
3 Université de Genève, Switzerland

Complete Photo-fragmentation of The Deuterium Molecule

by *Th. Weber[1,3,5], A. Czasch[1], O. Jagutzki[1], A. Müller[1], V. Mergel[1], A. Kheifets[2], E. Rotenberg[3], G. Meigs[3], M.H. Prior[3], S. Daveau[3], A.L. Landers[4], C.L. Cocke[5], T. Osipov[5], R. Díez Muiño[6], H. Schmidt-Böcking[1] and R. Dörner[1]*

All properties of molecules—from binding and excitation energies to their geometry—are determined by the highly correlated initial-state wavefunction of the electrons and nuclei. Details of these correlations can be revealed by studying the break-up of these systems into their constituents. The fragmentation might be initiated by the absorption of a single photon, by collision with a charged particle or by exposure to a strong laser pulse: if the interaction causing the excitation is sufficiently understood, the fragmentation process can then be used as a tool to investigate the bound initial state. The interaction and resulting fragment motions therefore pose formidable challenges to quantum theory.

A 'complete' description of the break-up of a molecule

In the article by Weber *et al.*, the coincident measurement of the momenta of both nuclei and both electrons from the single-photon-induced fragmentation of the deuterium molecule is reported. For each charged particle, the position of impact on the detector and the overall 'time of flight' are measured, and from them the initial momentum of all four particles can be deduced directly. Even more excitingly, in the case of hydrogen, the ions leave in opposite directions so quickly (compared with their rotational motion) that even the alignment of the molecular axis can be determined with respect to the polarization direction of the incident light. From the kinetic energy of the nuclei arriving at the detector, one can also obtain the Coulomb potential associated with their initial separation. Quantum mechanically, one maps the nuclear vibrational wave function onto the Coulomb potential to yield a kinetic-energy spectrum. All this gives a three-dimensional 'photograph' of the Coulomb explosion.

The results reveal that the correlated motion of the electrons is strongly dependent on the inter-nuclear separation in the molecular ground state at the instant of photon absorption. Although multiple scattering of the photoelectron wave could lead to a variation of the angular distributions, calculations for this particular system show that this effect, as a function of the inter-nuclear separation, is rather small. This is because the protons are relatively weak scattering centres and the long wavelength of the photoelectrons would require long paths within the molecular potential. The ultimate reason for such strong dependence should be then found in the initial-state wave function features. The experimental results are thus highly sensitive tests of the initial-state wave function and, consequently, of electron correlation effects in the initial state. ■

REFERENCE

T. Weber, A.O. Czasch, O. Jagutzki, A. K. Müller, V. Mergel, A. Kheifets, E. Rotenberg, G. Meigs, M.H. Prior, S. Daveau, A. Landers, C.L. Cocke, T. Osipov, R. Díez Muiño, H. Schmidt-Böcking, and R. Dörner, *Nature* **431**, 437 (2004).

1 Institut für Kernphysik, Universität Frankfurt, Germany
2 Research School of Physical Sciences and Engineering, Australian National University, Canberra, Australia
3 Lawrence Berkeley National Laboratory, Berkeley, California, USA
4 Department of Physics, Western Michigan University, Kalamazoo, Michigan, USA
5 Department of Physics, Kansas State University, Manhattan, Kansas, USA
6 Donostia International Physics Center and Unidad de Física de Materiales CSIC-UPV/EHU, San Sebastian, Spain

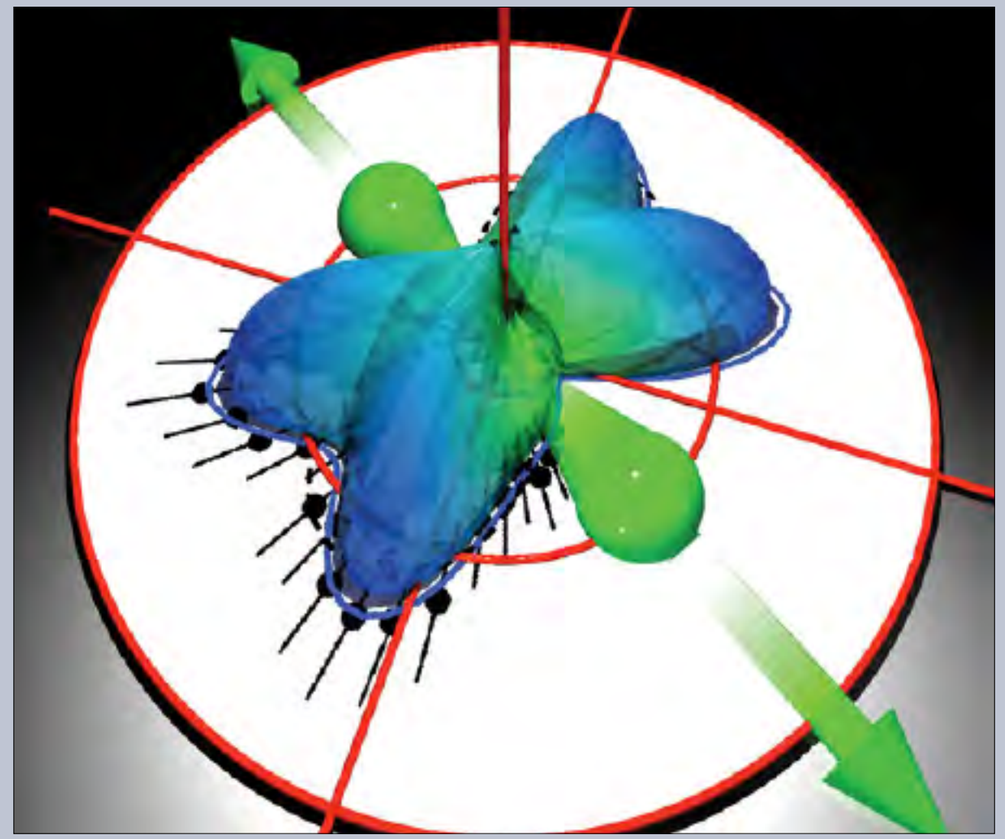

A three-dimensional 'photograph' of the double ionization of deuterium molecules, initiated by the absorption of photons.

The results reveal that the correlated motion of the electrons is strongly dependent on the inter-nuclear separation in the molecular ground state at the instant of photon absorption.

Contrast Reversal And Shape Changes of Atomic Adsorbates Measured with Scanning Tunneling Microscopy

by *F. Calleja[1], A. Arnau[2], J.J. Hinarejos[1], A.L. Vázquez de Parga[1], W.A. Hofer[3], P.M. Echenique[2,4] and R. Miranda[1]*

Systematic, quantitative comparisons between STM experiments and first principles simulations of O(2 x 2)/Ru(0001) have been performed. The shape of the atomic adsorbates in the images depends strongly on the tunnelling resistance and changes reversibly from circular (high resistance)to triangular (low resistance). In addition, after adsorption of oxygen on the STM tip we observe a contrast reversal on the surface, confirmed by extensive numerical simulations.

In many exciting areas, e.g. catalysis, high Tc materials and other complex transition metal oxides, it is important to identify metal and oxygen sites at surfaces in order to understand processes such as dissociation of molecules, spatial inhomogeneities in the superconducting gap or the role of impurities in the formation of striped phases. Although Scanning Tunnelling Microscopy (STM) images can in principle be used to characterize the topography of surfaces at the atomic level, they do not always simply reflect the real position of surface atoms. If we restrict ourselves to adsorbed oxygen layers or oxide surfaces, there are experimental reports claiming that, depending on the system and the state of the tip, either the O or the metal atoms are the bright features in the STM images. The observed shape of images is well understood in the case of isolated oxygen atoms adsorbed on metal surfaces. However, in dense, ordered arrays of adsorbed oxygen the situation is still unclear. Because the geometric and electronic structure of the surface, as well as the chemical state of the tip, play a role in determining the corrugation, contrast and shape of the image, it is necessary to perform *ab-initio* calculations to interpret properly the STM images. Here we report on a fundamentally new level of comparison between experiment and theory to clarify the role of the different parameters determining STM images like tip structure, sample voltage (V), tunneling current (I), and gap resistance (R). The measured series of STM images of the model system, O(2x2) superstructure of Oadsorbed on Ru(0001), is shown to be in quantitative agreement with first principles simulations. The geometric structure (adsorption site, interatomic distance, and relaxations) of the chosen system has been carefully characterized by low energy electron diffraction (LEED). The control parameters of the operation of the STM were systematically varied over a broad range (10 mV<V <1 V, 0:03 < t < 50 nA, 300 kOhm<R < 2 GOhm), and the ensuing changes were recorded and compared to simulated images. ■

REFERENCE

F. Calleja, A. Arnau, J.J. Hinarejos, A.L. Vázquez de Parga, W.A. Hofer, P.M. Echenique and R. Miranda, *Physical Review Letters* **92**, 206101 (2004).

1 Departamento de Física de la Materia Condensada, Universidad Autónoma de Madrid, Spain
2 Departamento de Física de Materiales UPV/EHU and Unidad de Física de Materiales CSIC-UPV/EHU, San Sebastian, Spain
3 Surface Science Research Centre, University of Liverpool, UK
4 Donostia International Physics Center, San Sebastian, Spain

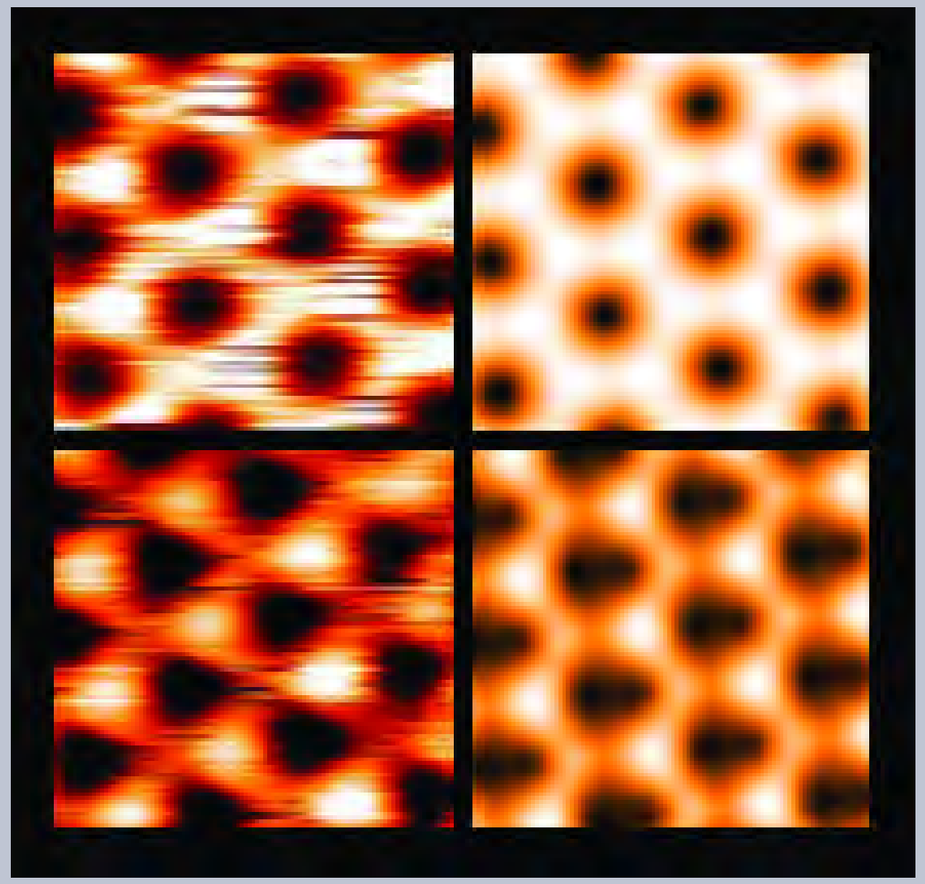

Comparison of experimental (left) and simulated (right) STM images of O(2x2)/Ru(0001). In both cases the sample voltage was -30 mV. The simulations have been performed with tunnelling currents of 0.03 nA (above) and 0.3 nA (below) and agree with the experiments.

Band Structure versus Dynamical Exchange-correlation Effects in Surface Plasmon Energy and Damping:

A First-Principles Calculation

by *V.M. Silkin*[1], *E.V. Chulkov*[1,2], *and P.M. Echenique*[1,2]

Since the introduction of surface plasmon (SP) concept remarkable progress has been achieved in the understanding of collective electronic excitations at metal surfaces. These excitations play an important role in such areas as surface dynamics including one-particle (electron and hole) dynamics, SP microscopy, SP resonance technology as well as in photonic applications. Here we report on the results of a first-principles parameter-free calculation of the dynamical surface response and surface plasmon properties of magnesium, a prototype simple metal. We demonstrate that band structure effects have a more profound impact on the SP properties than dynamical exchange correlation. Nevertheless to obtain better agreement with experiment the inclusion of proper exchange-correlation kernel is needed.

Surface plasmon properties are important in many areas of surface science.

Conceptually the SP, a fundamental surface mode, can be traced to the peaks of the imaginary part of the surface response function derived from the density response function of the interacting electron system. The density response includes both bulk and surface electrons and represents a very complex interplay between one particle electron states (band structure) and dynamical many-body correlations that affects both the SP energy and linewidth.

The difficulty in the description of a SP stems from a gradual transition of main driving forces from the long-wavelength limit to large momenta. In the long-wavelength limit the dielectric response is controlled by bulk properties, while for large momenta the main effect is due to the surface dielectric response. Thus for the proper description of the dispersion of the SP energy and width it is necessary to include both the bulk and surface electronic structure on the same footing. In parallel with the band structure the exchange-correlation effects were shown to be important for the description of bulk collective excitations in simple metals. For surface collective excitations the incorporation of dynamical exchange-correlations might be even more important than for bulk materials since unlike the bulk the surface charge density experiences fast variation at short distances from bulk values to zero in vacuum.

In the article by Silkin *et al.*, the results of the first parameter free ab initio calculation of the SP energy and linewidth for a real metal surface are reported. The relative impact of band structure and dynamical exchange-correlations on the SP is studied for Mg(0001). This surface can be viewed as a test one for the comparison of theoretical and experimental results because of the best quality of the Mg single crystal surface with respect to other simple metals. The results obtained show that even for such a nearly-free electron metal as Mg an excellent agreement with the experimental SP energy and linewith in a large range of 2D momenta is found if both the bulk and surface band structure on the same footing together with dynamical exchange-correlations are taken into account. The inclusion of band structure into the theory is crucial for the description of the correct behavior of the SP linewidth as well as of its anisotropy.

The calculated SP dispersion and linewidth for two symmetry directions of surface Brillouin zone are shown in the figure together with the experimental data. We also show there the results obtained from the jellium and one-dimensional potential models. From the comparison of these three models one can discriminate the relative role of such factors as modulation of one-electron potential in the direction perpendicular to the surface and full inclusion of three-dimensional band structure effects. In particular, the latter are crucial for the description of the SP linewidth, whereas jellium and one-dimensional potential models fail to reproduce the experimental linewidth for both small and large momenta. These effects account for the significant anisotropy predicted for the SP linewidth. They are also important for the energy dispersion of the SP. The inclusion of the momentum dependent exchange-correlations improves the theoretical results leading to excellent agreement with the experimental data. We have also found that lateral crystal local field effects have a negligible impact on the SP properties. Our conclusions about the relevance of band structure can be extended to systems with more complicated electronic structure than magnesium, for instance, to silver surfaces, which are of particular interest due to an unusual energy and dispersion of surface plasmon, and to palladium surfaces. ■

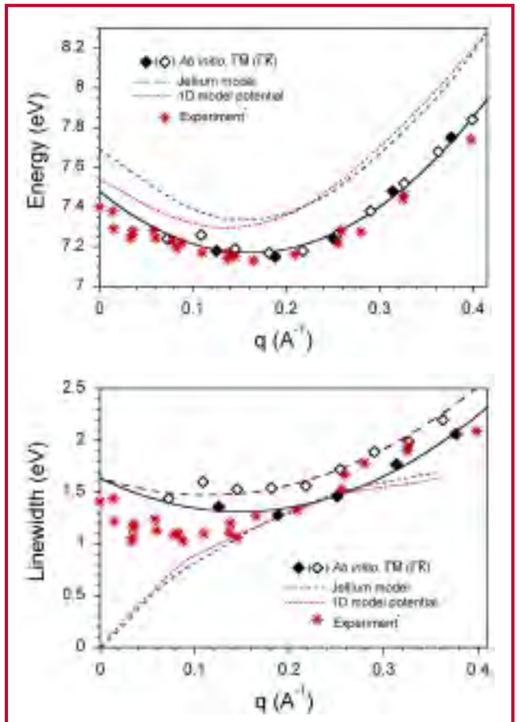

Surface plasmon energy (above) and linewidth (below) dispersions for Mg(0001) calculated with momentum-dependent kernel. Ab initio data for $\bar{\Gamma}\bar{M}$ ($\bar{\Gamma}\bar{K}$) direction of surface Brillouin zone are shown by the filled (open) diamonds. Solid (long dashed) line is the corresponding best fit to the data. Dashed (dotted) lines present the jellium model (1D model potential) diversions.

*P.D. Sprunger *et al.*, Surf. Sci. **269/270**, 551 (1992).

On the base of ab initio calculations it was demonstrated the relative importance of electron band structure and dynamical exchange-correlations in surface plasmon energy and its linewidth.

REFERENCE

V.M. Silkin, E.V. Chulkov, and P.M. Echenique, *Physical Review Letters* **93**, 176801 (2004).

1 Donostia International Physics Center, San Sebastián, Spain
2 Departamento de Física de Materiales UPV/EHU and Unidad de Física de Materiales CSIC-UPV/EHU, San Sebastian, Spain

Lifetimes of Excited Electrons in Fe and Ni: First-principle GW + T-matrix Theory

by *V.P. Zhukov*[1], *E.V. Chulkov*[1,2] *and P.M. Echenique*[1,2]

We develop a first-principle method for evaluating the life-times of spin-polarized excited electrons in ferromagnetic metals. The calculations show that the decay of low-energy excited states is expressly spin-dependent, in particular in Fe, where the life-time of spin-minority states is reduced due to the emission of magnons and spin-flip electron-hole pairs.

The spin-asymmetry of the excited electron life-times is a phenomenon that makes possible triggering of current in spintronic devices.

The spin-dependent lifetime of excited electrons in ferro-magnetic materials characterizes the ability of electrons to transfer the spin and is important for transport and spin accumulation phenomena employed in novel spintronic devices. It has been studied experimentally, by means of photoemission and time-resolved two-photon photoemission spectroscopy, and theoretically, mainly within semi-empirical models of scattering theory. However, present methods of evaluating the electronic lifetimes in ferromagnetic materials are still far from being perfect. In particular, an essential drawback of the semi-empirical theoretical calculations is the invocation of adjustable parameters and omission of some important mechanisms of the fast electron decay, such as the generation of electron-hole Stoner's pairs and spin waves.

A good alternative to the methods having the origin in scattering theory is provided by the *ab initio* methods based on many-body theory. The most important of them is the GW approach, where the lifetime is evaluated from the imaginary part of the electron self-energy. This approach is fairly good for systems with long-range screening, but it fails to describe short-range interactions and neglects the spin-flip scattering processes. In order to achieve a better understanding of the fast electron decay in ferro-magnetics, we extended the GW method by including the multiple scattering processes evaluated within the T-matrix approach.

We define T-matrix operator as a solution of Bethe-Salpeter equation

$$T_{\sigma_1\sigma_2}\langle 1,2|3,4\rangle = W(1,2)\delta(1-3)\delta(2-4) + W(1,2)\int d1'\,d2'\,K_{\sigma_1\sigma_2}\langle 1,2|1',2'\rangle T_{\sigma_1\sigma_2}\langle 1',2'|3,4\rangle$$

with the static RPA screened potential W. The kernel of this equation K is a product of two spin-dependent Green functions

$$K_{\sigma_1\sigma_2}\langle 1,2|1',2'\rangle = G_{\sigma_1}(1,1')G_{\sigma_2}(2',2)$$

In our calculations all the possible combinations of G have been taken into account: electron-electron, electron-hole and hole-hole Green's functions with equal and different spins. The most important T-matrix contribution to the self-energy is the direct term

$$\Sigma_{\sigma_2}(4,2) = -\sum_{\sigma_1}\int d1d3 G_{\sigma_1}(3,1)T_{\sigma_1\sigma_2}\langle 1,2|3,4\rangle$$

With $\sigma_1=\sigma_2$ we have high-order contributions to the non-spin-flip scattering, with $\sigma_1-\sigma_2$ this term provides spin-flip Stoner and spin-wave contribution to the self-energy. The pole frequencies of T-matrix with $\sigma_1-\sigma_2$ correspond to magnon energies. The explicit equations for the self-energy Σ^d in moment and frequency representation have been derived and implemented based on LMTO band-structure method.

1 Donostia International Physics Center, San Sebastián, Spain
2 Departamento de Física de Materiales UPV/EHU and Unidad de Física de Materiales CSIC-UPV/EHU, San Sebastian, Spain

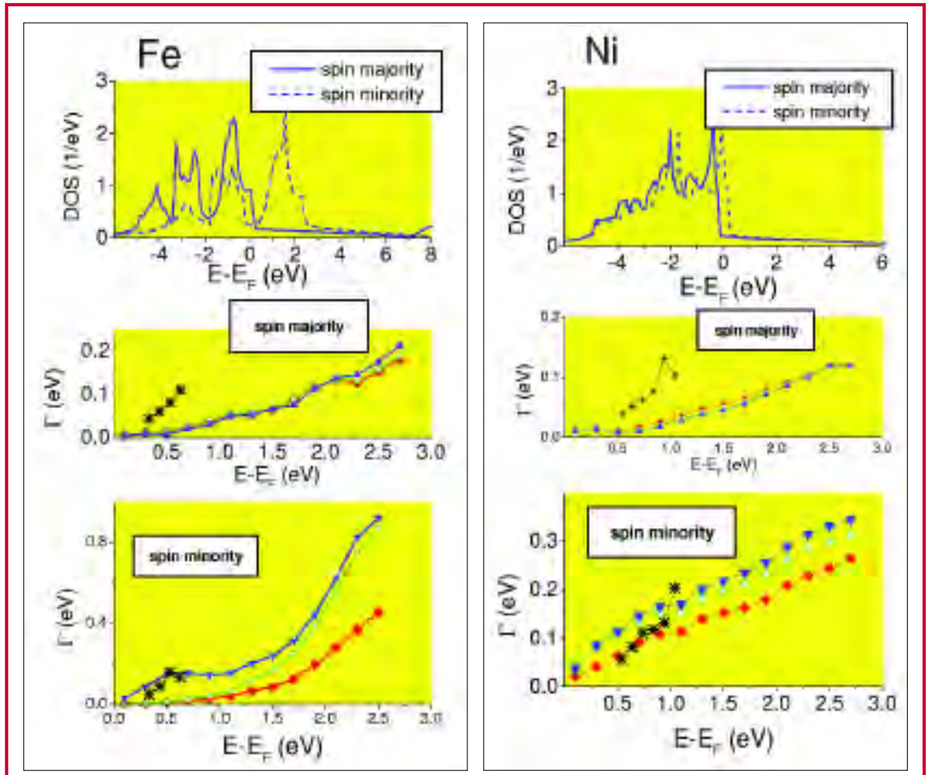

Figure: The calculated and experimental inverse lifetimes Γ of excited electrons in Fe and Ni. Solid red diamonds show the GW contribution to Γ, open green circles show GW+T non-spin-flip contribution, and red triangles show complete GW+T(non-spin-flip + spin-flip) Γ-values. Black stars show the experimental TR-2PPE inverse lifetimes.

In the Figure we show the calculated spin-projected densities of states (DOS) and inverse lifetimes (Γ) for Fe and Ni. For the spin-majority excited electrons both in Fe and Ni the contribution of T-matrix terms to Γ appear to be small. But for spin-minority electrons the effects of both spin-flip and non-spin-flip T-matrix terms are essential. For spin-minority electrons in Fe at excitation energy about 0.5 eV we observe a strong deviation of the GW+T results from the GW results. This deviation is associated with the scattering of excited electrons accompanied by the generation of spin waves and Stoner's electron-hole pairs. Similarly, the GW+T results for spin-minority electrons in Ni at excitation energy below 0.5 eV also diverge from GW results, but this divergence is associated mainly with the multiple electron-hole scattering without spin flips. The Γ values calculated for spin-minority electrons are in good agreement with experimental TR-2PPE data. But the theoretical Γ values for spin-majority states in Fe and Ni still remain lower than the experimental data. This is consistent with the fact that the experimental data include the effects of transport, electron-impurity and electron-phonon scattering. ■

REFERENCE
V.P. Zhukov, E.V. Chulkov and P.M. Echenique, *Physical Review Letters* **93**, 096401 (2004).

Strong Spin-orbit Splitting on Bi Surfaces

by *Yu. M. Koroteev[1,2], G. Bihlmayer[3], J.E. Gayone[4,5], E.V. Chulkov[1,6], S. Blügel[3], P.M. Echenique[1,6], and Ph. Hofmann[4]*

Understanding of electronic properties of surfaces of heavy semimetal materials is of paramount importance for transport phenomena due to the spin-orbit splitting of surface states (SS). Here we present the first ab initio calculation together with angle-resolved photoemission measurements of the SS bands on low-index surfaces of Bi. We show that the spin-orbit interaction leads to a strong splitting of the SS bands and profound modifications of the dispersion of these states and the corresponding Fermi surfaces. The implications of these findings can be important for the surface screening, surface spin-density waves, electron (hole) dynamics in surface states, quasiparticle interference, and for possible applications to the spintronics.

Surface states (SS) of a semimetal would give a prominent contribution to surface density of states that could make these systems interesting for applications in spintronics. The surfaces of the semimetal Bi are ideal to advance our understanding of spin-orbit coupling (SOC) on surfaces and how it manifests in experiments on electron-phonon coupling, electron and hole dynamics, possible formation of surface charge and spin density waves, and in quasiparticle interference. The strong SOC in low-dimensional structures of non-magnetic materials could also have applications like spin-filter devices.

We show by combining the results of first-principles calculations with high-resolution measurements of the electronic structure by ARPES that the SS on low-index surfaces of Bi exhibit a spin-orbit splitting of the bands which is by far stronger than any case reported so far. The results of the calculation agree well with experiment but only if the SOC is taken into account. We find that the SOC induced splitting is an essential ingredient for the description of the electronic structure: it profoundly changes the SS dispersion and the corresponding Fermi surfaces on all the Bi surfaces of interest.

Figure 1 shows the electronic structure of Bi(111) together with the projected bulk band structure calculated with and without

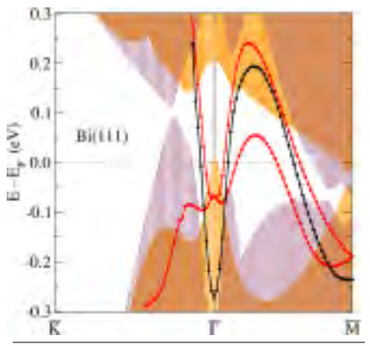

Figure 1. Surface states of Bi(111) calculated without (black) and with (red) spin-orbit splitting included. The shaded areas show the projection of the bulk bands obtained without (violet) and with (yellow) SOC and their superposition (brown).

SOC. Without SOC, we find a parabolic $\bar{\Gamma}$ SS located in the nonrelativistic energy gap. Around $\bar{\Gamma}$ this SS band gives an electron FS hexagon. With the SOC included it results in a spin-splitting of the SS in all the symmetry directions and leaves it degenerate only at $\bar{\Gamma}$ and at $\bar{M}$. Around $\bar{\Gamma}$ this relativistic SS is degenerate with bulk states and shows less clear surface character. The lift of the spin degeneracy leads to radical change of the surface FS: 1) The radius of the FS hexagon is

1 Donostia International Physics Center, San Sebastian, Spain
2 Institute of Strength Physicsand Materials Science, Russian Academy of Sciences, Tomsk, Russia
3 Institut für Festkörperforschung, Forschungszentrum, Jülich, Germany

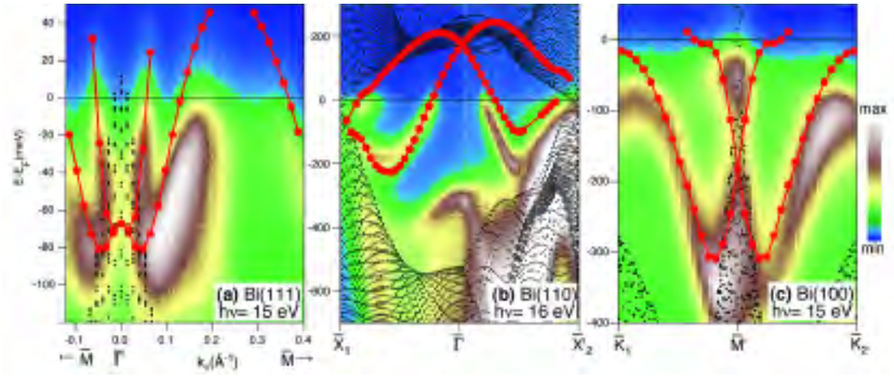

Figure 2. Calculated and measured electronic structure in the vicinity of two high symmetry points on three surfaces of Bi. (a) $\bar{\Gamma}$ on Bi(111), (b) $\bar{\Gamma}$ on Bi(110), and (c) $\bar{M}^1$ on Bi(100). The small black dots are the projected bulk band structure. The red filled circles are the calculated surface state energies, thin red line is a guide to the eye. The photoemission intensity is linearly scaled from dark blue (minimum) to white (maximum).

smaller by 30% compared to the nonrelativistic calculation; 2) In the $\bar{\Gamma}$ $\bar{M}$ symmetry directions the hole lobes are formed. Another remarkable feature of Bi(111) is the very strong anisotropy of the SOC: it is 0.2 eV in the $\bar{\Gamma}$ $\bar{M}$ direction and even more in the $\bar{\Gamma}$ $\bar{K}$ one.

The strong spin-orbit splitting is verified by comparing the calculations with the experimental results. Figure 2 shows the calculated electronic structure for Bi surfaces together with experimental data. In Figure 2(a) we find excellent agreement for the two split SS for Bi(111). Figure 2(b) also shows the situation for Bi(110). In contrast to Bi(111) this SS is unoccupied at and has negative effective electron masses that lead to the formation of the hole FS pocket around $\bar{\Gamma}$. The scenario of a very steep band and a flatter one near $\bar{\Gamma}$ can be found on Bi(100).

The SOC-induced splitting should have some important consequences for the physical properties of the Bi surfaces, in particular, for the screening. In the Lindhard picture of screening, the susceptibility (q) is given by an integral over all processes where an electron hops between an occupied state and an unoccupied state separated by q. In a two-dimensional situation this type of screening can lead to a CDW-type instability only when there are 'nested' elements of the FS, separated by q. Such a situation exists for Bi(111) where the FS of the electron pocket around $\bar{\Gamma}$ is hexagonal. Ast and Hoöchst have recently shown (*Physical Review Letters* **90**, 016403 (2003)) that the leading edge of the energy distribution curves at the Fermi level crossing shifts discontinuously as a function of temperature, indicating the formation of a CDW. However, when we take into account the spin of the states involved in the alleged formation of the CDW, the electron hopping across the FS would have to undergo a spin-flip because of the split nature of the bands. This makes the occurrence of a CDW very unlikely.

The spin-orbit splitting in surface bands on the Bi surfaces can also have drastic consequences for electron and hole dynamics in surface states. In particular, the surface response function should include all the spin-flip processes between the split surface bands with different spin direction. It can lead to the formation of surface spin-density waves even in cases when the nesting at the surface FS does not occur. The spin-orbit splitting should also lead to different hole (electron) lifetimes in surface states compared to that for the non-split surface state. This is due to both the surface response function that now includes spin-flip processes and to a different phase space factor. The surface state spin-orbit splitting can also affect the electron-phonon (e-ph) coupling on the Bi surfaces. We would like to note that the existence of spin split surface states also permits a spin-wave mediated e-ph interaction. ■

The surface response function should include all the spin-flip processes between the split surface bands with different spin direction.

REFERENCE
1 Yu. M. Koroteev, G. Bihlmayer, J.E. Gayone, E.V. Chulkov, S. Blügel, P.M. Echenique, and Ph. Hofmann, *Physical Review Letters* **93**, 046403 (2004).
2 J.I. Pascual, G. Bihlmayer, Yu. M. Koroteev, H.-P. Rust, G. Ceballos, M. Hansmann, K. Horn, E.V. Chulkov, S. Blügel, *Physical Review Letters* **93**, 196802 (2004).

4 Institute for Storage Ring Facilities, University of Aarhus, Denmark
5 Centro Atomico Bariloche and CONICET, Bariloche, Argentina
6 Unidad de Física de Materiales CSIC-UPV/EHU and Departamento de Física de Materiales UPV/EHU, San Sebastián, Spain

Controlling the Conductance of Single-walled Carbon Nanotubes: Anderson Localization

by *C. Gómez-Navarro[1], P. J. de Pablo[1], J. Gómez-Herrero[1], B. Biel[2], F. J. García-Vidal[2], A. Rubio[3], and F. Flores[2]*

Carbon nanotubes are a good realization of one dimensional crystals where basic science and potential nanodevice applications merge. For the case of electronic circuits based on carbon nanotubes, the influence of disorder and defects is of fundamental relevance in the performance of the device (e.g. the density of defects can change the transport regime from ballistic regime to either weak or strong localization). Defects can be present in as-grown carbon nanotubes therefore, it is crucial to understand the properties of these defects in order to conquer their detrimental effects, but also because controlled defect introduction may be used to tune nanotube properties in a desired direction.

Observation of Anderson localisation at room temperature in irradiated carbon nanotubes

Quantum theory dictates that for a one dimensional conductor with defects weak localization effects emerge when the "phase coherence length" is larger than the localization length, L_0. For very long wires ($L>>>L_0$), the electron transport is a diffusive process controlled by localization, with the electrons hopping between neighbouring localized states. However, if L is not too large (for L about 3-10 L_0) and the inelastic interaction is weak, the wire resistance is controlled by the phase-coherent electron propagation, falling into the strong localization regime in which the resistance increases exponentially with the length of the wire. This regime is the one addressed here as in nanotubes the dephasing length can easily be longer than the localization length, which is the basic requirement for achieving Anderson localization.

Experimentally, a metallic AFM tip was used to measure the current vs. voltage characteristics of the nanotubes as a function of the distance between the metallic AFM tip, used as mobile electrode, and a fixed macroscopic gold electrode (see figure). By measuring the electrical resistance of the same metallic nanotube after successive irradiations we were able to map the resistance as a function of the nanotube length. Our data shows that the resistance increases exponentially with length at scales L ≥ 500 nm (see inset in the figure). The length scale at which this exponential behavior is observed could be reduced substantially by irradiation with Ar^+ ions, indicating that it is caused by Anderson localization. Simulations demonstrated that mainly di-vacancies contributed to the exponential conductance drop induced by irradiation (di-vacancies appear in about 30-40% of the Ar^+ impacts).

We used a first-principles Local Orbital Density Functional method to calculate the relaxation around the defects and transport characteristics. The advantage of this approach is that it provides a means of calculating the conductance using standard Green-function techniques derived for tight-binding Hamiltonians but now with first-principles accuracy allowing the calculation of the electronic properties of very long nanotubes (up to several microns long) with an arbitrary distribution of defects immersed on them providing a quantitative comparison between theory and experiments. In the figure we show the calculated mean value of the room T resistance (as a result of an average over 15 random cases) as a function of the carbon nanotube length for different d's.

1 Departamento de Física de la Materia Condensada, Universidad Autónoma de Madrid, Spain
2 Departamento de Física Teórica de la Materia Condensada, Universidad Autónoma de Madrid, Spain
3 Departamento de Física de Materiales UPV/EHU and Donostia International Physics Center, San Sebastian, Spain

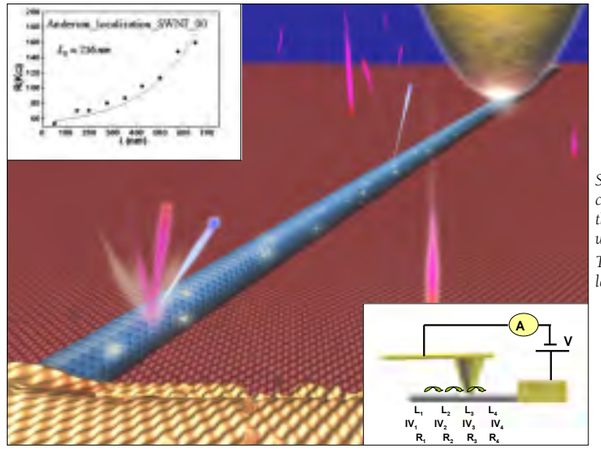

Scheme of the experimental set-up showing a gold covered AFM tip, the macroscopic gold electrode, the SWNT, the irradiation with Ar atoms and the used circuit.
The top inset shows one low-voltage-resistance vs. length, clearly exhibiting Anderson localisation.

The calculated resistance fits a universal curve once it is plotted in terms of the number of defects (N) instead of the total length (L). The inset shows that calculated room T localization length, L_0 exhibit two distinct regimes: i) for lower defect density (i.e., large values of *d, d*>5 nm), L_0 depends linearly with *d*, ii) For higher defect density (small values of *d*), L_0 saturates. In all our measurements the defect density is below 0.15% corresponding to case (i).

To highlight our findings, we have shown the extreme importance of defects (in particular di-vacancies) on the low-bias conducting properties of single-walled carbon nanotubes irradiated with an Ar^+ ion beam: only a 0.03% of di-vacancies produce an increment of three orders of magnitude in the resistance of a 400 nm carbon nanotube segment. Our theoretical calculations support this conclusion, indeed for a (10,10) carbon nanotube we have found: (i) the transition between the ballistic and the localization regimes appears for a small number of di-vacancies (about 3–5). (ii) For a higher number of defects the system shows localization, reducing the number of effective channels from two (ballistic) to one. (iii) At zero T, the nanotube conductance shows strong fluctuations. The net effect of a finite T is to wash out those strong fluctuations. We remark that, in spite of the disappearance of the fluctuations, the exponential behavior is still preserved at room T. Besides its fundamental relevance, this work opens new paths to tailor the electrical properties of future nanotube devices using ion irradiation. It also suggests the possibility of using these devices as radiation detectors and points out the limits of performance of carbon nanotubes in the presence of radiation. Whether interaction effects — that is, Tomanaga–Luttinger-liquid type of correlations — play a role has to be resolved by future investigation. ■

Temperature washed out the quantum fluctioatins in the conductance but not the localisation phenomena.

REFERENCES

C. Gómez-Navarro, P. J. de Pablo, J. Gómez-Herrero, B. Biel, F. J. García-Vidal, A. Rubio, and F. Flores, Tuning the conductance of single-walled carbon nanotubes by ion irradiation in the Anderson localization regime, *Nature Materials* **4**, 534-539 (2005).

B. Biel, F.J. García-Vidal, A. Rubio and F. Flores, Anderson localization in carbon nanotubes: defect density and temperature effect, *Physical Review Letters* **95**, 266801 (2005).

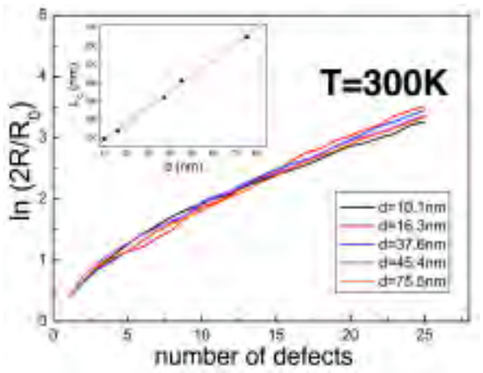

Interplay Between Electronic States and Surface Structure in Ag Layers

by *F. Schiller[1], J. Cordón[1], D. Vyalikh[2], A. Rubio[3,4,5], F.J. García de Abajo[5] and J. E. Ortega[3,4,5]*

We investigate the interplay between surface electronic states and geometric structure in the Ag/Cu triangular dislocation network. Experiments involve Scanning Tunneling Microscopy and Angle Resolved Photoemission with synchrotron radiation, and these are compared with model theoretical calculations. Distinct one-monolayer (incommnesurate) and two-monolayer (commensurate) lattices suggest the presence of structural instabilities that give rise to two-dimensional Fermi surface nesting and gap opening. Simple elastic/electronic energy arguments explain the experimental observations.

The interplay between electronic surface states and structure is observed in a Ag monolayer

Nanostructures exhibit exotic electronic and magnetic properties due to their reduced dimensions. New phases appear that do not have a bulk counterpart, e.g., *incommensurate* phases, which can drive structural phase transitions. They are particularly important in the context of cooperative phenomena like superconductivity, or spin and charge density wave transitions. Incommensurate phases appear upon Fermi surface nesting, i.e. by slightly forcing the crystal lattice to make the Fermi surface fit the Brillouin zone. This allows a band gap to open up at the Fermi energy, thereby lowering the electronic energy. The group at the Nanophysics Laboratory have recently provided clear evidence for Fermi surface nesting and surface state driven stabilization of the 2D incommensurate 9.5x9.5 Ag monolayer (ML) grown on Cu(111)[1].

The 1 ML Ag/Cu(111) system is an interesting example of layer-by-layer growth in large (13%) mismatched materials. In this case, the Ag monolayer wets the substrate and forms a compressed, out-of-registry 9.5x9.5 superstructure, with a lattice compression of 1.1% with respect to the bulk Ag(111) plane. The question arises why the system favors the out-of-registry 9.5x9.5 structure in this case, instead of, for instance, the registry 9x9 with only 0.4% lattice compression, which is indeed observed in 2 ML Ag/Cu(111). Using high resolution, angle resolved photoemission Schiller et al. have observed a Fermi gap to open in the out-of-registry 9.5x9.5 ML, by contrast to a gapless surface band observed in the registry 9x9 superstructure of the 2 ML Ag film. This result suggests that the compresed 9.5x9.5 incomensurate phase may be stabilized by such Fermi surface gap, and hence by the subsequent electronic energy gain.

Figure 1(a) shows the Scanning Tunneling Microcopy (STM) image for a ML thick Ag stripe grown on Cu(111) at 300 K. The work was carried out in the VT Omicron set-up in San Sebastian. The Ag is deposited on top of a Cu(111) single crystal held at 150 K and then shortly annealed to 300 K. This procedure leads to a hexagonal (see the Fourier

1 Departamento de Física Aplicada I, UPV/EHU, San Sebastian, Spain
2 Institut für Festkörperphysik, Technische Universität Dresden, Germany
3 Departamento de Física de Materiales UPV/EHU, San Sebastian, Spain
4 Donostia International Physics Center, San Sebastian, Spain
5 Unidad de Física de Materiales CSIC-UPV/EHU, San Sebastian, Spain

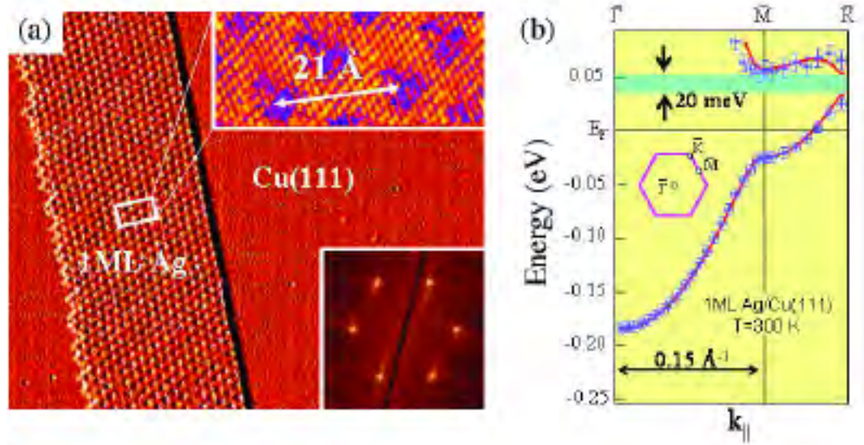

(a) STM image showing a monolayer-thick, Ag stripe grown on Cu(111). A 9.5x9.5 hexagonal pattern of lattice constant d=21Å is visible (Fourier transform in the lower inset). The upper inset shows a closer, atomically-resolved view. The structure is actually defined by a Ag close-packed layer that wets an array of triangular dislocation loops in the Cu(111) substrate.
(b) Surface bands for 1 ML Ag /Cu(111) measured with angle resolved photoemission (photon energy 21.2 eV). Fermi surface nesting leads to the large 80 meV Fermi gap that opens up at the bar point of the hexagonal structure. The surface band displays an absolute 20 meV slightly above the Fermi energy.

The group at the Nanophysics Laboratory have recently provided clear evidence for Fermi surface nesting and surface state driven stabilization of the 2D incommensurate 9.5x9.5 Ag monolayer (ML) grown on Cu(111).

transform in the lower inset) pattern with an average 21 Å lattice constant, i.e., a 9.5x9.5 reconstruction with respect to the Cu substrate. The atomically resolved image in the top inset probes the microscopic structure, namely a Ag close-packed layer that wets the array of triangular misfit dislocation loops induced in the Cu substrate. Figure 1(b) shows the surface band dispersion for 1 ML Ag/Cu(111) measured with angle resolved photoemission along the symmetry directions of the hexagonal structure. The photoemission experiments were performed with a Scienta 200 high-resolution angle resolved hemispherical analyzer in the University of Dresden. Fermi surface nesting at leads to the 80 meV band gap that opens up at that point.

The band dispersion measured across the whole Brillouin zone in Figure 1(b) shows strong modifications of the, otherwise, free-electron-like band of noble metals. In particular we observe a full 20 meV band gap slightly above the Fermi energy. The presence of this gap, which suggests exotic transport properties in the system, has been confirmed in a model calculation using a hexagonal array of triangular potential barriers[3]. On the other hand, using the band structure measured in Figure 1(b), the electronic energy difference between out-of-registry (9.5x9.5) and the registry (9x9) structures can be straightforwardly calculated. This gives a negative 0.31 meV/atom value, which indeed competes with the positive 0.48 meV/atom elastic energy difference, i.e., the energy needed to compress the Ag monolayer from the (9x9) to the (9.5x9.5) close-packed structures[2]. ■

REFERENCE
1 F. Schiller, J. Cordón, D. Vyalikh, A. Rubio, and J.E. Ortega, *Physical Review Letters* **94**, 016103 (2005).
2 F. Schiller, J. Cordón, D. Vyalikh, A. Rubio, and J.E. Ortega, *Physical Review Letters* **96**, 029702 (2006).
3 F.J. García de Abajo *et al.* (to be published).

Direct Observation of the Electron Dynamics in the Attosecond Domain

by *A. Föhlisch*[1], *P. Feulner*[2], *F. Hennies*[1], *A. Fink*[2], *D. Menzel*[2], *D, Sánchez-Portal*[3], *P.M. Echenique*[3] *and W. Wurth*[1]

Two theoreticians from DIPC, Dr. Daniel Sánchez-Portal and Prof. Pedro M. Echenique, have recently participated in a study of the dynamics of electrons at surfaces that was published in *Nature*[1]. The aim of the study was to answer the following question:

How long does it take for an electron to hop between atoms?

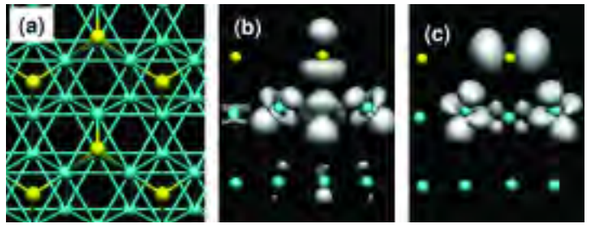

For the studied system, an order structure of sulphur atoms deposited on the Ru(00001) surface, it turned out to be a very short time of about 320 attoseconds or 320x10^{-18} seconds. This is one of the shortest processes ever measured in solid state physics. However, the measurement was performed directly in time domain. This was only possible due to the use of an appropriate "clock", which in this case was chosen as the decay time of an internal hole of the sulphur atom. This technique is known as "core-hole-clock" spectroscopy, and in this work its resolution was significantly increased by the use of Coster-Kronig transitions. The experimentalist used X-ray pulses to excite an electron of sulphur to an electronic state where it is unstable and tends to move away from the sulphur atom into the ruthenium substrate. In this excited state the sulphur atom is also unstable against a Coster-Kronig autoionization process. This decay process takes place in a similar (although somewhat longer) time scale than the sulphur-ruthenium hopping, and produces a distinct signal that can be clearly measured. In fact, the autoionization produces two different signals (peaks) depending on whether the initial electron has already left the atom or not when the autoionization takes place. The key is then to measure the relative intensities of these two peaks, and the sulphur-ruthenium hopping time can be extracted from this intensity ratio. This measurement has been performed by a group of researchers from several German laboratories, the work being directed by Prof. Wilfried Wurth from Hamburg University.

The researchers from the DIPC simultaneously developed a method to calculate the charge-transfer times of electrons initially residing in excited states of adsorbates to the corresponding metallic substrates. The calculations were based on state-of-the-art electronic structure calculations, using the so-called density-functional theory, to compute the details of the combined adsorbate-substrate system. These results were then combined with calculations of the bulk of the substrate material to obtain the Green's function of the semi-infinite system using recursive techniques. The calculations are thus based on a realistic description of the electronic structure of both systems, the substrate and the adsorbate, and the interaction between them. This allows to make predictions about the charge-transfer rates in different systems and to understand in detail the dynamics of electrons at surfaces. This scheme was then applied to study the sulphur covered ruthenium substrate. It was confirmed that for the particular set-up used in the experiments, the charge-transfer time was indeed well below 1 femtosecond (10^{-15} seconds) and close to the measured 320 attoseconds. They also predicted the variation of the observed charge-transfer time with the polarization of the excitation light (see the figure). This effect still waits for experimental verification.

1 Institut für Experimentalphysik, Universität Hamburg, Germany
2 Physik Department E20, Technische Universität München, Germany
3 Unidad de Física de Materiales CSIC-UPV/EHU, Donostia International Physics Center and Departamento de Física de Materiales UPV/EHU, San Sebastian, Spain

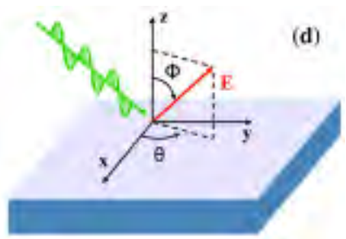

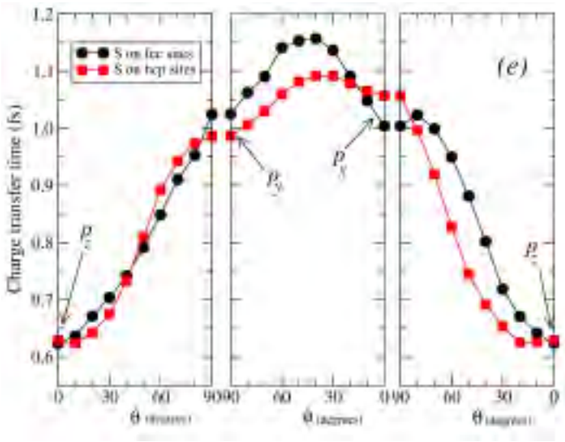

*Figures. Panel (**a**) shows the c(4x2) Ru(0001) surface. Different excitation geometries translate to different initial electronic wavepackets. The initial wavepackets are constructed by projecting linear combinations of the sulphur 3p states onto the relevant energy window. Panels (**b**) and (**c**) show the electron density associated with "pz" and "px" orbitals. Panel (**e**) shows the charge transfer time as a function of the symmetry of the initial wavepacket (i.e. the field polarization in the experiment, see panel (**d**)).*

The calculations were based on state-of-the-art electronic structure calculations, using the so-called density-functional theory, to compute the details of the combined adsorbate-substrate system.

This theoretical method has also been applied to unveil the importance of the elastic contribution to the total widths of the quantum well states at alkali overlayers on Cu(111)[2], allowing to explain the spectra obtained with scanning tunneling spectroscopy (STS) in such surfaces. More recently the case of Ar monolayers on Ru(0001) have been also studied[3], finding again values and trends for the charge-transfer times in good agreement with the core-hole-clock experiments.

Dr. Sánchez-Portal and Prof. Echenique, and their experimental colleagues are treating to extend their results to resolve the different behavior of electrons with different spins in magnetic systems. This can provide crucial information for developing future electronic devices based on the spin of the electrons, a field known as 'spintronics'. Charge-transfer is also key to many biological processes such as photosynthesis. ■

REFERENCE

1 A. Föhlisch, P. Feulner, F. Hennies, A. Fink, D. Menzel, D, Sánchez-Portal, P.M. Echenique, and W. Wurth, *Nature (London)* **436**, 373 (2005).
2 C. Corriol, V. M. Silkin, D. Sánchez-Portal, A. Arnau, E. V. Chulkov, P.M. Echenique, T. von Hofe, J. Kliewer, J. Kröger, and R. Berndt, *Physical Review Letters* **95**, 176802 (2005).
3 D. Sánchez-Portal, D. Menzel and P.M. Echenique, to be published.

Potential Energy Landscape of a Simple Model for Strong Liquids

by *A.J. Moreno*[1,2], *F. Sciortino*[2,3], *I. Saika-Voivod*[2], *E. Zaccarelli*[2,3], *E. La Nave*[2,3], *S.V. Buldyrev*[4], *and P. Tartaglia*[2]

We introduce a minimal model exhibiting all the phenomenological features characterizing strong behavior in network-forming liquids. The statistical properties of the potential energy landscape can be computed for the first time with arbitrary precision even in the low temperature limit. A degenerate disordered ground state and non-Gaussian statistics for the distribution of local minima are the landscape signatures of strong liquid behavior. Differences from fragile liquid behavior are attributed to the presence of a discrete energy scale, provided by the particle bonds, and to the intrinsic degeneracy of topologically disordered networks.

In this work we aim to clarify the statistical properties of the PEL of strong liquids.

The structural relaxation time of a supercooled liquid increases over 13 orders of magnitude with decreasing temperature. At some given temperature, equilibration is not possible within laboratory time scales and the system becomes a glass. In 1969, Goldstein proposed to view a supercooled liquid as a point moving in the high-dimensional landscape of its potential energy. At low temperatures the system is located in deep valleys of the potential energy landscape (PEL). Short-time vibrational dynamics correspond to motions within a valley. Long-time structural relaxation occurs via motion between neighbouring valleys separated by high energy barriers.

In the Stillinger-Weber approach, the PEL is partitioned into basins around its local minima. The total entropy is obtained as a sum of a *configurational* contribution, given by the distribution and multiplicity of the local minima, and a *vibrational* contribution, related to the configurational volume available within the basins. Nowadays, the PEL is a key concept in the understanding of the glass transition problem. In particular, numerical investigations provide strong correlations between geometrical properties of the *static* PEL and *dynamic* features of supercooled liquids.

A glass-forming liquid is classified as *fragile* if the temperature dependence of its structural relaxation time on approaching the glass transition shows large deviations from Arrhenius behavior. If no deviations are observed, the liquid is classified as *strong*. Polymeric or low molecular weight organic liquids, where interactions do not show a marked directional character, are fragile. Inorganic liquids forming open network structures are strong.

In this work[1] we aim to clarify the statistical properties of the PEL of strong liquids. We carry out simulations on a system of particles interacting via a spherical hardcore plus a finite square-well potential, with a constraint on the maximum number (four) of bonded neighbours per particle. As a consequence of the finite square-well interaction, particles form a connected network of reversible bonds. The population of broken bonds decreases with decreasing temperature. By construction, the energy of the ground state (the fully bonded network) is unambiguously known. Contrary to simulations in real systems, the ground state can be reached *in equilibrium* and no extrapolations are needed in the calculation of thermodynamic functions at low temperatures.

1 Donostia International Physics Center, San Sebastian, Spain
2 Dipartimento di Fisica, Universitá di Roma "La Sapienza", Rome, Italy
3 INFM-CRS-SOFT, Rome, Italy
4 Department of Physics, Yeshiva University, New York, USA

Local minima are identified as topologically different bonding patterns. The basin associated to a given minimum corresponds to the configurational volume that can be explored by deforming the bonding pattern without breaking or forming bonds. With this definition, vibrational and configurational entropies can be formulated for the first time in an exact way, and the accuracy in their numerical evaluation is just limited by the precision of statistical averages.

The universal dynamic features shared by strong liquids, as Arrhenius behavior of the diffusivity, and weak stretching for dynamic correlators, are reproduced by this minimal model. The evaluation of the configurational entropy provides several striking features. In contrast to observations in fragile liquids, the distribution of local minima strongly deviate from Gaussian behavior. This feature is consistent with PEL analysis in atomistic models of silica (the archetype of strong behavior), and originates from the lower energy cut-off and the *discrete* energy scale provided by the inherent network of bonds.

The configurational entropy *per particle* takes a finite value in the limit of low temperature (see figure). This feature is confirmed by displaying the configurational entropy vs. the energy. The fact that the ground state (the fully bonded network) is reached in equilibrium excludes the possibility of ulterior changes in thermodynamic functions. According to this result, strong liquids are characterized by a degenerate ground state, originating from the exponential number of topologically distinct patterns the fully bonded network can adopt.

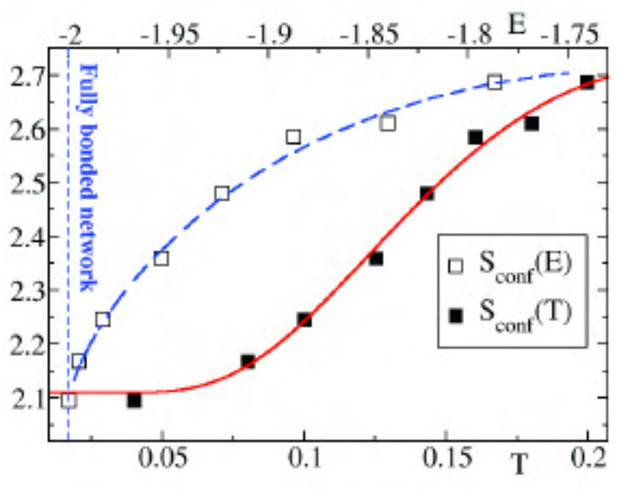

The configurational entropy per particle takes a finite value in the limit of low temperature.

We like to mention that, in a different physical context, this model provides a way of forming low-density arrested states (gels) without encountering phase separation[2]. Due to the constraint in the maximum number of bonds per particle, energy differences between particles located at the bulk and at the surface of the spanning clusters are strongly reduced, and the phase-separated region is largely shrunk. This result is relevant for gel-forming systems showing localized and directional interactions, as patchy colloids or some proteins. ■

REFERENCES

1 A.J. Moreno, S.V. Buldyrev, E. La Nave, I. Saika-Voivod, F. Sciortino, P. Tartaglia, and E. Zaccarelli, *Physical Review Letters* **95**, 157802 (2005).

2 E. Zaccarelli, S.V. Buldyrev, E. La Nave, A.J. Moreno, I. Saika-Voivod, F. Sciortino, and P. Tartaglia, *Physical Review Letters* **94**, 218301 (2005).

Why is Polycarbonate An Excellent Engineering Polymer?

by *A. Alegría*[1,2], *O. Michelena*[1], *J. Colmenero*[1,2,3]

The molecular origin of the excellent mechanical properties of bisphenol-A polycarbonate has been debated since more than 20 years without any definitive consensus so far. One of the more recent and controversial results on this topic was found when the phenylene ring dynamics was investigated by using neutron scattering. These measurements provided the first experimental confirmation of phenylene ~90° rotation, which was predicted to occur from numerical calculations on the small molecule analogues of polycarbonate. We have shown that this particular molecular motion is of utmost importance on the secondary dielectric relaxation of polycarbonate and being therefore deeply connected with its excellent properties.

It is likely you have realized that plastics are present everywhere in your daily life. You can find these materials in your computer, printer, furniture, car... This is because engineering polymers are durable, light, cheap, and have good mechanical and thermal properties making them suitable for a huge number of applications. Polycarbonate (PC) is one of the most widely used engineering thermoplastics. The interesting ultimate mechanical properties of PC are related to the ability of it to accommodate a stress, which involves highly activated molecular motions including those of the phenylene rings. That is why considerable efforts have been made to identify the molecular origin of the so-called secondary relaxations in PC and other related polymers. Though the existence of these processes and their main general features are established for many decades, their microscopic origin remained elusive. Traditionally these polymers have been studied by mechanical relaxation techniques and nuclear magnetic resonance. Only very recently, a detailed and systematic neutron scattering investigation of the phenylene ring dynamics in engineering thermoplastics, has demonstrated that only in PC, phenylene rings performs ~90º rotations, in addition to the π-flip motions generally observed in this family of polymers. In fact, numerical calculations on the small molecule analogues of polycarbonate already predicted phenylene ~90º rotations to occur.

Thus, taking these results into account, we have revisited the dielectric relaxation behavior of polycarbonate by new careful measurements over extremely broad ranges of both temperatures (50 - 350 K) and frequencies (10mHz-1GHz), looking in very detail for the effects of molecular orientation on the dielectric signal of the sample. The first comparison between the results obtained in the oriented sample with that of unoriented PC revealed a non-uniform reduction of the dielectric losses, the part of the response more reduced by orientation having the dynamic characteristics of the phenylene ~90º rotations as determined from neutron scattering. In addition, a further careful analysis of the dielectric losses of PC has allowed to evidence that the second main contribution to the dielectric relaxation has the same dynamic characteristics than those of phenylene ring π-flips. These results imply that the dielectric relaxation of PC arises from the strong coupling between the phenylene ring motions and those of the carbonate unit (see below), being this latter motion the ultimate responsible of the observed dielectric signal.

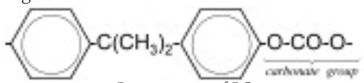

Repeating unit of PC

Namely, although the pheylene π-flips should not alter the molecule geometry much because of the high symmetry of the rings, the molecular distortions occurring during the phenylene π-flips would induce significant rearrangements of the surrounding units and particularly of the carbonate group. On the other hand, the calculations on small molecules analogues of PC showed that phenylene ~90º rotations have to be accompanied by similar jumps of the adjacent carbonate units, hence contributing very noticeably to the dielectric relaxation. In addition to these main contributions, the dielectric relaxation of PC presents a weak and faster component that resulted directly connected with small angular oscillations of the phenylene rings. This molecular assignment is illustrated in Figure 1. It allows rationalizing the 'anomalous' behaviors found in the dielectric relaxation of PC:

i) It allows the understanding of why molecular orientation reduces less the slowest component of the dielectric relaxation. The high symmetry corresponding to a phenylene π-flip yields the ring after the π-flip to be at the same position as it was before, and therefore, only short living fluctuations of the environment are necessary. On the other hand, after the phenylene ~90º rotation, the ring needs to have the corresponding available room, which obviously is much more difficult in a sample having molecular orientation, where the rings tend to stack parallel to each other.

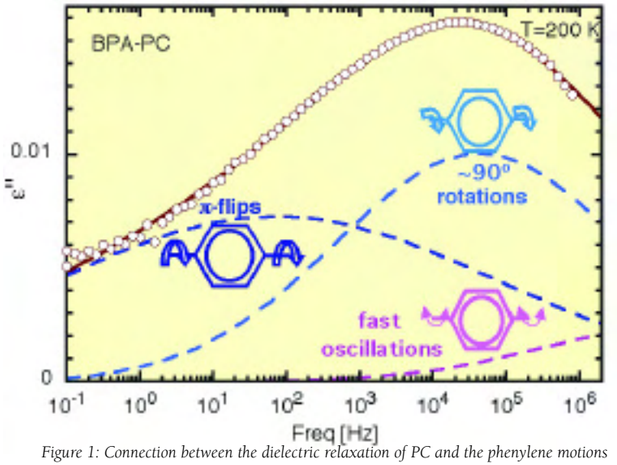

Figure 1: Connection between the dielectric relaxation of PC and the phenylene motions

ii) The same arguments also explain why when decreasing temperature there is a strong reduction of the contribution of phenylene ~90º rotations to the dielectric relaxation. The higher density would strongly diminish the probability of finding long living holes for accommodate a ring after a ~90º rotation. In fact, the marked temperature dependence of the main dielectric contributions makes the shape and average time of the dielectric relaxation to show unusual temperature behavior.

These results lead us to conclude that the phenylene ~90º rotations are of utmost importance in relation to the excellent mechanical properties of PC. This is further supported by the fact that it is just at the ductile-brittle transition temperature where the probability of phenylene ~90º rotations to occur starts increasing rapidly. ■

The interesting ultimate mechanical properties of PC are related to the ability of it to accommodate a stress, which involves highly activated molecular motions including those of the phenylene rings.

REFERENCES
1 O. Mitxelena, J. Colmenero and A.Alegría *Journal of Non-Crystalline Solids* **351**, 2652 (2005).
2 A. Alegría, O. Mitxelena, and J. Colmenero. *Macromolecules* **39**, 2691(2006).

1 Departamento de Física de Materiales UPV/EHU, San Sebastian, Spain
2 Unidad de Física de Materiales CSIC-UPV/EHU, San Sebastian, Spain
3 Donostia International Physics Center, San Sebastian, Spain

Dynamic Confinement in Miscible Polymer Blends

by *A.-C. Genix[1], M. Tyagi[1], A. Arbe[2], F. Alvarez[2,3], J. Colmenero[1,2,3], L. Willner[4], D. Richter[4], B. Frick[5], J.R. Stewart[5]*

Neutron scattering measurements with space/time resolution have provided first direct experimental evidence at a molecular level of confinement effects in a miscible polymer blend. These are induced by the freezing of the component with higher glass transition temperature T_g and are a direct consequence of the dynamic heterogeneity characteristic of polymer mixtures. Fast localized dynamics are observed for the low-T_g component, with associated jump lengths of about 2-3Å. These results have been corroborated by complementary fully atomistic molecular dynamics simulations.

Extreme dynamic heterogeneity in diluted blends leads to confinement effects with enhanced local dynamics in the glassy state.

By now the dynamic heterogeneity is a well established feature of polymer blends. It refers to the observation, even in a thermodynamically miscible system, of two different characteristic timescales for segmental relaxation, each of them corresponding to each component. A large experimental effort has been devoted to the phenomenological characterization of this property and nowadays models based on the concept of self-concentration successfully capture the main ingredient leading to two distinct timescales. Dynamic heterogeneity is magnified in highly asymmetric blends. This asymmetry can refer to the blend composition (diluted in one component) or also to the dynamics of the pure polymers (very different glass-transition temperatures, T_g). Thus, an intriguing question arises: what happens under such extreme conditions that, as a consequence of the strong dynamic heterogeneity, the slow component is completely frozen on the timescale of the segmental motions of the fast component?

First experimental evidences of a non-equilibrium situation were reported from dielectric spectroscopy studies for poly(vinyl methyl ether) (PVME) in blends with high concentration of polystyrene (PS). The behavior found, strongly, suggested the emergence of confinement effects for the fast component (PVME) when PS approaches its glass transition in the blend. However, dielectric spectroscopy does not provide the spatial information necessary to fully characterize the dynamics of the fast component. The required space/time resolution at a molecular level is offered by neutron scattering techniques, which allow in addition the selective study of one of the blend components by deuteration of the other polymer chains.

Direct microscopic observation of the confined dynamics was realized by neutron scattering on poly(ethylene oxide) (PEO) in blends with poly(methyl methacrylate) (PMMA) and poly(vinyl acetate) (PVAc) with low concentrations of PEO. The T_gs of the homopolymers differ by almost 200K (PEO/PMMA) and 100K (PEO/PVAc). In the high momentum transfer (Q) region, the characteristic times obtained for PEO in both mixtures clearly deviate from the expected momentum transfer dependence in the melt (Q^{-4}) and become nearly constant, suggesting the occurrence of localized motions (see Figure 1). From the Q-range where this flattening is observed, a spatial length scale of about 2 Å could be deduced for such hopping processes. Moreover, we note that in the low-Q regime, for the lowest temperatures investigated (below the T_g of the slower component) the Q-dependence is much steeper than that corresponding to Rouse dynamics. This would imply that the large-scale motions are clearly slowed down with respect to the equilibrium behavior, and could be considered as a signature of the freezing of the global chain dynamics as a consequence of the confinement of PEO motions by the rigid matrix formed by the other component in the blend.

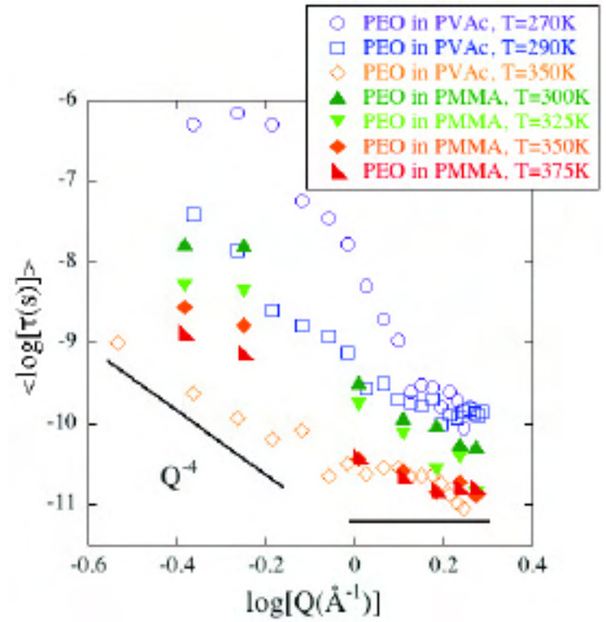

Momentum transfer dependence of the timescales obtained by neutron scattering for PEO in blends with PMMA and PVAc

In a complementary way, molecular dynamics simulations were performed in the blend PEO/PMMA with 10% PEO content. As can be seen in Figure 2, the occurrence of jumps in PEO is supported by the simulation results, which allow direct insight in real space. The development of a second maximum in this function reveals hopping processes with associated jump lengths of the order of 3 Å (see the distance between the two maxima for the longest time), in very good agreement with the neutron scattering results.

Thus, we have observed and characterized the confined motions taking place in a polymer surrounded by other rigid chains. The plasticization induced by blending, together with the emergence of such confinement effects leading to a fast local dynamical process, might provide a new route to tailor the properties of new commodities based on already existing materials. ■

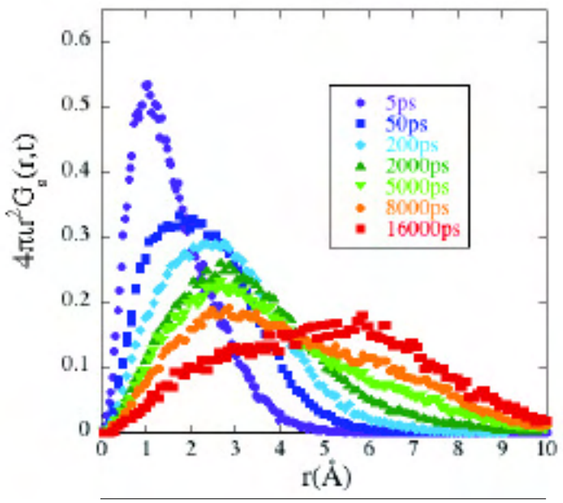

Radial self-correlation function obtained from the MD-simulations for PEO in the PMMA-blend at different times

REFERENCES
A.C. Genix, A. Arbe, F. Alvarez, J. Colmenero, L. Willner, D. Richter, *Physical Review E* **72**, 031808 (2005).
M. Tyagi, A. Arbe, J. Colmenero, B. Frick, J.R. Stewart, *Macromolecules* **39**, 3009 (2006).

1 Donostia International Physics Center, San Sebastian, Spain
2 Unidad de Física de Materiales CSIC-UPV/EHU, San Sebastian, Spain
3 Departamento de Física de Materiales UPV/EHU, San Sebastian, Spain
4 Institut für Festkörperforschung, Forschungszentrum Jülich, Germany
5 Institut Laue-Langevin, Grenoble, France

Polybutadiene Dynamics Close to the Glass Transition: Hop, hop! We're freezing!

by *J. Colmenero[1,2,3], A. Arbe[2], F. Alvarez[1,2], A. Narros[1], M. Monkenbusch[4], D. Richter[4]*

The potential of (carefully validated) fully atomistic MD-simulations is demonstrated by unravelling the puzzling situation concerning the dynamics of polybutadiene close to the glass transition. The identification in real space of hopping processes has put into a context the variety of experimental observations for this polymer. This was only possible by selective scrutiny of the different atomic species. Though linked through chain connectivity, polybutadiene hydrogens located in the different structural units preserve their own dynamical identities close to the glass transition.

The controversial results from experiments close to the glass transition reflect the rich local dynamics at microscopic level.

Many original works in polymer physics have been performed on the "in principle" simple and archetypal polybutadiene, -[CH_2-CH=CH-CH_2-]$_n$. In particular, this was the favorite sample for neutron scattering experiments during many years, yielding quite a number of relevant observations, mainly by neutron spin echo (NSE). For instance, it was the first polymer where NSE measurements at the first structure factor peak revealed the structural (α) relaxation. Later, during a pioneering NSE excursion in the intramolecular region, an additional process was found, that was active in the neighborhood of the glass transition (T_g = 178 K). The nearly identical temperature dependencies of the dielectric β-relaxation and the dynamic structure factor at the second peak (intrachain) suggested a common molecular origin for both processes. However, a difference of more than two orders of magnitude in the associated characteristic timescales prevented a definitive connection between them (see Figure 1). In the mean time, the relaxation map of polybutadiene has become even more puzzling, since two additional processes were reported from light scattering experiments (see Figure 1).

Trying to shed some light in the molecular origin of all these processes, we have performed fully atomistic MD-simulations on this system at 200 K. Our cubic cell contained one chain of 130 monomers with a microstructure (39 % cis; 53 % trans; 8 % vinyl units) similar to that of the real sample. Two big advantages of fully MD-simulations are: (i) to easily allow monitoring different atomic species and (ii) to directly access the real space. We have exploited both in this work and an example of the outcome is shown in Figure 2. First of all, we realize that the main feature of the hydrogen motions at timescales close to the nanosecond is the predominance of localized processes —the radial distribution functions develop a more or less evident second maximum at about 2.7 Å. It is worth noting that this feature is hidden in the reciprocal space accessed by the experiments. The second observation is the markedly heterogeneous behavior: each kind of hydrogen evolves in a different way! The most diverse motions seem to be carried out by the hydrogens attached to the double bonds in the cis and trans units (see the insert of Figure 2).

1 Departamento de Física de Materiales UPV/EHU, San Sebastian, Spain
2 Unidad de Física de Materiales CSIC-UPV/EHU, San Sebastian, Spain
3 Donostia International Physics Center, San Sebastian, Spain
4 Institut für Festkörperforschung, Forschungszentrum Jülich, Germany

The real space data of these two species were fitted by considering simultaneous occurrence of hopping processes and sublinear diffusion due to the structural relaxation. We obtained the following results: The trans hydrogens undergo jumps of a well defined length, 2.5 Å, while the cis hydrogens show jump distances broadly distributed around the same value. For both kinds of atoms we obtained broad distributions of characteristic times that can be attributed to the inherent disorder in our polymer. Interestingly, the average timescale observed for the cis atoms is much longer than that characterizing the trans motions. They have been displayed in Figure 1. The comparison with previous experimental results is revealing: (i) the fastest motions of the trans units are probably responsible for the light scattering observations; (ii) the dielectric β-relaxation is produced by the localized motions carried out by the cis group —very plausible, since the dipole moment in polybutadiene is associated to this unit—; and (iii) NSE delivers an average of both motions. This is also logical, since the dynamic structure factor relates to all atoms in the sample, carbons and deuterons, and therefore an intermediate timescale is observed. Thus, the controversial polybutadiene experimental observations are just the result of rich local dynamics at microscopic level. Finally, concerning the subdiffusive component of the motions, we found a perfect agreement with the expectation for the contribution of the α-relaxation (see Figure 1), strongly supporting the consistency of the framework and the analysis of the data. ■

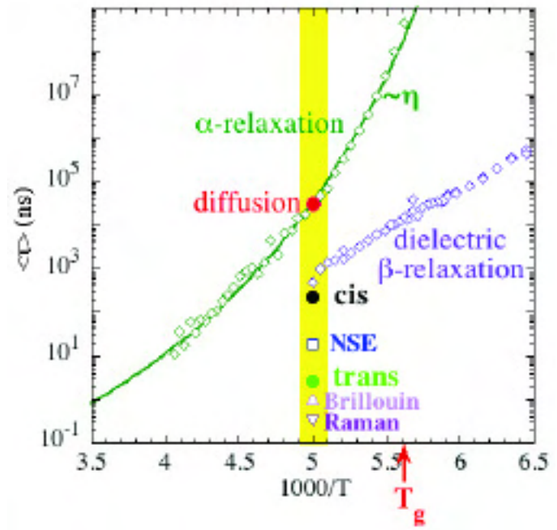

Variety of timescales identified for polybutadiene by different experimental methods (empty symbols) and the processes observed by the simulations (full dots).

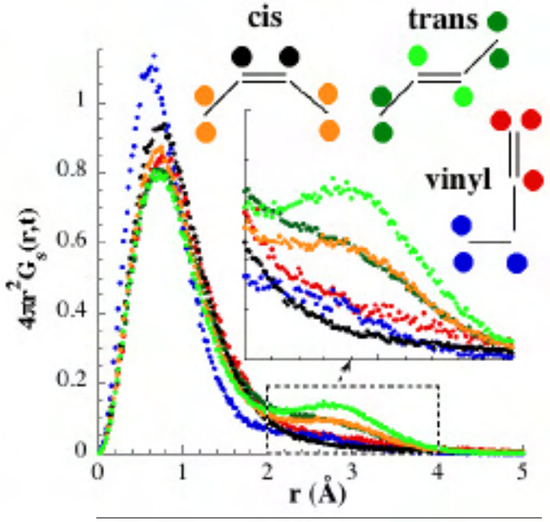

Radial self-correlation function at t = 1 ns obtained from the MD-simulations for the different hydrogens in polybutadiene (the colors indicate for which atom).

REFERENCE
J. Colmenero, A. Arbe, F. Alvarez, A. Narros, M. Monkenbusch, D. Richter, *Europhysics Letters* **71**, 262 (2005).

The Surroundings Really Matter... Also for Polymer Motion

by *D. Cangialosi[1], G.A. Schwartz[1], A. Alegría[2,3], J. Colmenero[1,2,3]*

The segmental dynamics of a polymer, giving rise to the glass transition, is generally altered when this polymer is mixed to another one with different mobility. This is mainly due to the fact the polymer "senses" the local environment around it up to a scale of several nanometres. Thus, the characteristic volume involved in the motion will possess an effective concentration in this component that is higher than the bulk concentration of the blend. This picture can be successfully incorporated in one of the available theoretical approaches describing the dynamics of glass-formers: the Adam-Gibbs theory relating the mobility to the number of available configurations.

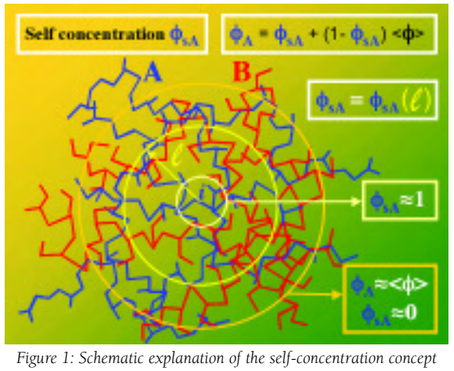

Figure 1: Schematic explanation of the self-concentration concept

The last decades have seen a growing interest in the study of miscible polymer blends due to the potential application of these systems. Furthermore, the study of the segmental dynamics of these systems offers the possibility of extracting fundamental information on the nature of the glass transition.

The main feature of the dynamics of polymer blends is the speed-up or slow-down of the dynamics of one polymer, when this is surrounded by another polymer with relatively different dynamics. The effect of the other component of the blend is strongly related to the length scale involved in the dynamics. The characteristic length scale determines the effective concentration experienced by a given polymer segment. This feature, which is known as self-concentration effect, is moreover enhanced by chain connectivity. The essential features of this concept are explained in Figure 1 and can be summarised as follows: when a volume is centred on the basic structural unit of one of the polymers of the blend, the effective concentration will be different from the macroscopic one. Two extremes cases are possible: i) if this volume equals the volume of the basic structural unit, then the effective concentration is one, and ii) if, on the other hand, this volume is large enough, then the effective concentration equals the macroscopic one.

To rationalize the effect of blending on the dynamics of polymers, we have proposed a model based on the combination of the self-concentration concept with the Adam-Gibbs (AG) theory, relating the characteristic time for the segmental relaxation with the number of configuration the system can explore. This

1 Donostia International Physics Center, San Sebastian, Spain
2 Departamento de Física de Materiales UPV/EHU, San Sebastian, Spain
3 Unidad de Física de Materiales CSIC-UPV/EHU, San Sebastian, Spain

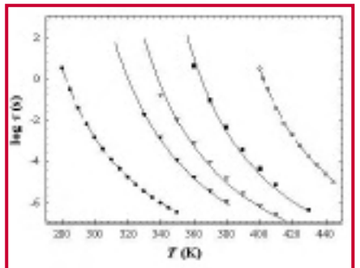

Figure 2: Logarithm of the relaxation time vs. temperature for pure PoClS (open circles), PS700 (filled circles) and for PoClS in blends with PS700 with weight percentages: 25% (filled triangles), 50% (open triangles) and 75% (filled squares). The solid lines are the fittings of the model to the blends experimental data.

number, namely the configurational entropy, can be obtained from calorimetric measurements. Furthermore, we have exploited the concept of a growing length scale with decreasing temperature implicit in the AG theory that proposes a correlation between the configurational entropy and the characteristic length scale, such that at high temperatures the characteristic volume is small but it increases as temperature is reduced. The model relies on just one fitting parameter, namely the proportionality constant between the length scale and the configurational entropy, which is unreliably determined from the AG theory. As this parameter is polymer specific, one can predict the dynamics of miscible polymer blends once this parameter has been determined studying the dynamics of other polymer blends as well as polymer-solvent mixtures. To sum up, once the only unknown parameter of the model is obtained indirectly, the dynamics of miscible polymer blends can be fully predicted starting from the knowledge of the dynamics and the thermodynamics of the pure components of the blend.

We have obtained these results by measuring the segmental dynamics of several miscible polymer blends and of the pure components of the blends. This was done employing broadband dielectric spectroscopy (BDS), which is capable of measuring selectively the mobility of all those systems possessing relaxing dipoles. Moreover, precise determination of the specific heat of the pure components of the blends has been performed by modulated differential scanning calorimetry (MDSC). This allowed evaluating the configurational entropy of the pure components of the blend as required by the model.

As an example, we show in Figure 2 the segmental dynamics of poly-o-chlorostyrene (PoClS) in polystyrene oligomer (M_n=700 g/mol) (PS700). The two polymers display a rather large dynamic contrast being the glass transition temperature (T_g) of PoClS equal to 402K and that of PS700 equal to 280K. Moreover, PoClS possesses a far larger dipole moment than PS700 and, therefore, the dielectric response can be attributed to the segmental relaxation of PoClS in the blend. From inspection of Figure 2, we clearly observe that the dynamics of PoClS is accelerated by the presence of the more mobile PS700. The acceleration is enhanced for blend with larger PS700 content. These qualitative results are a clear indication that the surrounding plays a decisive role in affecting the dynamics of polymers. These features are quantitatively captured by our model as indicated by the solid lines in Figure 2.

Our results also indicate a prominent role of self-concentration and provide an estimation of the length scale involved in the segmental relaxation of polymer blends. This is universally found to be between 1 and 3 nanometers. ■

REFERENCE

D. Cangialosi, G.A. Schwartz, A. Alegría, J. Colmenero, *Journal of Chemical Physics* **123**, 144908 (2005).

Once the only unknown parameter of the model is obtained indirectly, the dynamics of miscible polymer blends can be fully predicted starting from the knowledge of the dynamics and the thermodynamics of the pure components of the blend.

Water and Polymers: A New Route to Approach the Dynamics of Biological Water

by *S. Cerveny*[1], *J. Colmenero*[1,2,3], *A. Alegría*[2,3]

Water is a substance that fascinates everyone, newborn babies or scientists alike, and it is essential for all life on earth. However, despite its importance and widespread interest we do not fully understand the dynamic behavior of water in confining environments, as it is the case of biological systems. In this work we face this problem by studying water dynamics in mixtures with water-soluble synthetic polymers. The results give new insight on the dynamics of confined water in more complex environments such as biological materials.

Biological macromolecules —proteins and DNA— are physiologically inactive without water.

While many aspects of structure and dynamics of bulk water can be regarded as reasonably understood at present, the same is not true for the water which is found in interfacial or restricted environments, such as the surface of proteins or micelles. Water at the surface of a protein defines a molecular layer that has been termed "biological water" or "first hydration shell" and exhibits unique characteristics. In addition, there is a second hydration shell formed by loosely bounded water molecules. However, biological systems are extremely complex since movements of the host materials mask and can directly affect the water dynamics. Contrarily, synthetic polymers (such as poly (vinyl methyl ether)) offer the possibility to study the water dynamics in a well controlled environment since the polymeric chains often remain frozen in the temperature range where the water dynamics is relevant and the presence of the polymer acts as inhibitor of crystallization.

We have investigated the properties of PVME/H_2O mixtures by both dielectric and calorimetric methods. Our experiments have been focused on the water dynamics in the low temperature range (150-200 K) where the PVME matrix remains essentially immobile since the glass transition temperature (T_g) of dry PVME is around $T_g \approx 250$K. We considered the hydration water dynamics at several polymer concentrations (from concentrated solution up to 50 wt%). In addition, dielectric relaxation spectroscopy is suited for the investigation of the H-bond rearrangement dynamic due its ability to monitor the motion of water dipole.

Our recent work confirms that different hydration shells can be also found in hydrated polymers at low temperatures. In the case of PVME-water mixtures, at water content lower than 34 wt%, water molecules interact strongly with the polymer matrix, which suppress its translational motions and limit their reorientation ability (first hydration shell). This is notice for both the impossibility of crystallization and a dielectric relaxation weaker than that expected from water molecules without orientational restrictions (Figure 1).

1 Donostia International Physics Center, San Sebastian, Spain
2 Unidad de Física de Materiales CSIC-UPV/EHU, San Sebastian, Spain
3 Departamento de Física de Materiales UPV/EHU, San Sebastian, Spain

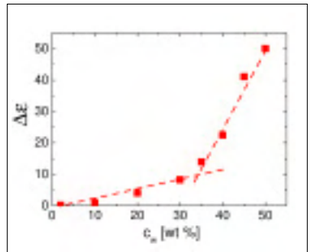

Figure 1: Dielectric relaxation strength of PVME aqueous solutions for water concentration up to 50% wt. A non-monotonous increase with water content is found defining clearly when water molecules start forming the second hydration layer.

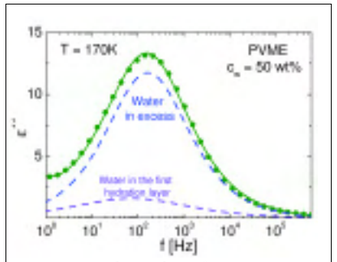

Figure 2: Dielectric loss of a PVME-water solution (c_W=50 wt%). Note the decomposition of the total dielectric signal (solid line) in a contribution attributed to the first hydration shell water molecules (dotted line) and another from loosely bounded water (dashed line).

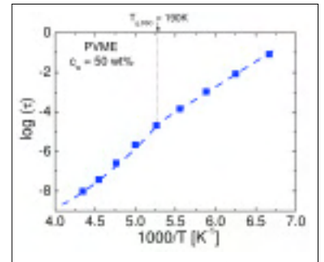

Figure 3: Relaxation time of a PVME-water solution (c_W=50 wt%). Note the crossover between Arrhenius and VFT behavior at $T_{g,DSC}$.

In contrast, at high water concentration all the hydrophilic sites are already occupied and, therefore, there are water molecules which are surrounded only by other water molecules. This excess water behaves more like-bulk water: it tends to crystallize easily and has a stronger contribution to the dielectric relaxation reflecting weaker restrictions for reorientations. Thus, the measured dielectric signal can be modelled as a sum of two different contributions: one related with the water molecules H-bonded to the polymer (or water in the first hydration shell and obtainable from the spectra with c_W=30 wt%) and the other one related to the water in excess or water in second hydration level (Figure 2).

Another interesting feature of water dynamics is that it shows an Arrhenius temperature dependence at the low temperatures, where the polymer matrix remains frozen, and crosses-over to the behavior typical of glass formers above this temperature (Figure 3).

Finally, it is important to note that the feature showed for PVME is also valid for other water soluble polymers [such as poly(vinyl pyrrolidone)] and for small molecules (such as ethylene glycol or propylene glycol and its oligomers). ■

Our recent work confirms that different hydration shells can be also found in hydrated polymers at low temperatures.

REFERENCE

S. Cerveny, J. Colmenero, A. Alegría, *Macromolecules* **38**, 7056 (2005).